LA-UR-03-9308

Semiclassics of the Chaotic Quantum-Classical Transition

Benjamin D. Greenbaum,[1] Salman Habib,[2] Kosuke Shizume,[3] and Bala Sundaram[4]

[1]*Department of Physics, Columbia University, New York, New York 10027*
[2]*T-8, Theoretical Division, Los Alamos National Laboratory, Los Alamos, NM 87545*
[3]*Institute of Library and Information Science, University of Tsukuba, 1-2 Kasuga, Tsukuba, Ibaraki 305-8550, Japan*
[4]*Department of Physics, University of Massachusetts, Boston, MA 02125*

We elucidate the basic physical mechanisms responsible for the quantum-classical transition in one-dimensional, bounded chaotic systems subject to unconditioned environmental interactions. We show that such a transition occurs due to the dual role of noise in regularizing the semiclassical Wigner function and averaging over fine structures in classical phase space. The results are interpreted in the novel context of applying recent advances in the theory of measurement and open systems to the semiclassical quantum regime. We use these methods to show how a local semiclassical picture is stabilized and can then be approximated by a classical distribution at arbitrary times. The general results are demonstrated explicitly via numerical simulations of the chaotic Duffing oscillator.

PACS numbers: 05.45.Mt,03.65.Sq,03.65.Bz,65.50.+m

I. INTRODUCTION

Since the birth of quantum physics, the boundary between the quantum and classical descriptions of nature has been the cause of much controversy and debate. Although few people now believe in the required existence of a "large" classical world in which quantum mechanics is somehow embedded, even for those that believe in the primacy of a full quantum description, the identification of the actual physical processes that allow a quantum dynamical system to be approximated – in some limit – by a classical dynamical system often remains less than clear-cut.

Initially the problem of quantum-classical correspondence was phrased in the context of understanding how the fundamental "subatomic" laws of quantum physics could possibly be compatible with a "macroscopic" world which, to a very good degree of approximation, evolves according to classical Hamiltonian dynamics and lacks (classically) bizarre quantum characteristics such as interference and entanglement [1]. This view was famously, if somewhat vaguely, canonized in Bohr's Correspondence Principle. In common parlance, the phrase is typically invoked to mean one of three related, but not identical, subjects: the existence of a formal analogy between certain preferred classical dynamical variables and quantum observables; the limit of large quantum numbers, large action or small $\hbar$, possibly in some combination; or the extent to which classical and quantum dynamical evolutions agree, in the spirit of Ehrenfest's theorem and semiclassical dynamics.

The last two interpretations, which are the principal foci of this paper, often overlap with one another but are not identical. Additionally, since quantum and classical mechanics are fundamentally different in their notion of what defines a physical system state, comparisons between the two must be made carefully so as to be maximally consistent with these basic notions. As an example, the position and momentum expectation values of a quantum harmonic oscillator evolve exactly according to the classical Liouville equation, and given an initial distribution acceptable both classically and quantum-mechanically, the two theories give identical results. However, if we consider a quantum energy eigenstate of the oscillator and attempt to compare it to a classical orbit at the same energy, ad hoc reasoning must be utilized to eliminate rapid quantum oscillations about the classical values. This is one example of the singular nature of the semiclassical limit ($\hbar \to 0$).

A similar situation exists in the two-slit experiment and other simple dynamical systems [2]. However, the topics of interference elimination and dynamical agreement are often related insofar as decreasing the size of $\hbar$ will usually have the effect of altering the scale of quantum interference while simultaneously improving the time scale of agreement of classical and quantum expectation values when they are not already identical (e.g., the trivial linear case above), as is the case for all nonlinear systems. The spirit of these ideas is that quantum mechanics should be approximated by classical mechanics in some appropriate macroscopic limit so as not to contradict measurable classical observations.

The problems associated with the semiclassical limit become seriously compounded when one transitions from linear to nonlinear systems. While a prescient set of quantum founding fathers, notably Einstein and Born, quickly noticed that semiclassical quantization schemes were not well-defined for nonintegrable systems [3], the scope of these difficulties is most apparent when they are viewed in the context of the last forty years of advances in classical nonlinear dynamics.

Theoretical insight and experimental observation of chaotic systems has made it clear that classical chaos is a real world phenomena that quantum theory should

reproduce to within experimental accuracy. However, closed-system classical mechanics and quantum dynamics have fundamentally incompatible dynamical symmetries. Any nonlinear dynamical system will, after a finite time, fail the conditions of Ehrenfest's theorem, meaning that quantum expectation values cannot obey classical predictions at long times and quantum dynamics will therefore not preserve the classical symplectic dynamical symmetry [4]. If a nonlinear system is also chaotic, this only hints at the full scope of the problem. The symplectic classical phase space evolution allows chaotic systems to generate fine structures at infinitesimally small scales, whereas quantum evolution preserves interference effects and consequently does not possess a notion of local phase space structures at sub-$\hbar$ scales. If, in a formal sense, the only way for quantum dynamics to recover classical dynamics for long time scales is to take $\hbar$ all the way to zero, this (singular) limit runs into the difficulty of generating increasingly wild phase oscillations in the wavefunction rather than a smooth (limiting to delta-function) classical trajectory picture. Viewing this problem from the other direction, i.e., constructing an approximation to quantum dynamics from classical trajectories, the result is a short-time disagreement between the semiclassical and classical evolution due to a proliferation of nonlocal interference effects, followed by the failure of the semiclassical approximation at longer, but still finite time scales [5, 6]. Yet another way to illustrate the difficulty is to note that closed bounded quantum systems have quasi-periodic dynamics and hence, technically, can never be chaotic, no matter what the value of $\hbar$ happens to be, as long as it is not zero. (This prompted some early investigators in the field to wonder if quantum mechanics had to be modified in order to produce chaos [7].) As a consequence of these obstructions, chaotic systems have emerged as a testing ground for whether or not quantum-classical correspondence is truly a valid concept, and, if so, how it should be properly phrased and addressed.

A parallel set of experimental developments, particularly in the last twenty years, have also strongly suggested the need for a more refined view of the quantum-classical transition (QCT). The border between the macro-world of classical mechanics and the micro-world of quantum physics has become blurred by technological, observational, and theoretical progress. Precision measurements in nanomechanics, atomic and molecular optics, and quantum information processing and communication have probed mesoscopic regimes, necessitating a careful analysis of the relative merits of using a classical or quantum description since the systems studied are neither "very large" nor "very small" (in a sense to be quantified later). In a quite different realm, recent observations of the cosmic microwave background and the large-scale distribution of galaxies have strongly supported the notion that quantum fluctuations are the primary mechanism for the formation of large scale structures in the Universe [8], thus demonstrating that crude criteria of "microscopic" vs. "macroscopic" are no longer sufficient as an underlying basis for a serious study of the QCT.

A consensus is forming that spanning the gap between the above problems and the correspondence principle requires a robust understanding of open quantum systems and quantum measurement [9]. Any experimentally relevant system is, by definition, a *measured* system which interacts with its environment, if only through a meter which may or may not record information. A quantum measurement differs from a classical one in at least two regards: (i) the intrinsic barrier imposed by the uncertainty principle on the precision of phase space information a meter can extract and (ii) the more severe manner in which the subsystem becomes entangled with its environment. Due to this entanglement, quantum measurement is generically associated with an irreducible disturbance on the observed system (quantum "backaction"). This being so, if our aim is that measurement yield dynamical information – rather than strongly influence dynamics – the desired measurement process must yield a limited amount of information in a finite time. Hence, simple projective (von Neumann) measurements are clearly not appropriate because they yield complete information instantaneously via state projection. But this fundamental notion of measurement can be easily extended to devise schemes that extract information continuously [10].

The basic idea is to have the system of interest interact weakly with another (e.g., atom interacting with an electromagnetic field) and make projective measurements on the auxiliary system (e.g., photon counting). Because of the weak interaction, the state of the auxiliary system gathers very little information regarding the system of interest, and therefore this system, in turn, is only perturbed slightly by the measurement backaction. Only a small component of the information gathered by the projective measurement of the auxiliary system relates to the system of interest, and a continuous limit of the measurement process can be taken.

One may then study the master equation for the evolution of a subsystem density matrix conditioned on its measurement record. The master equation can be further "unraveled" into nonlinear stochastic trajectories for a pure state, the so-called quantum trajectories [11]. An average over the pure states gives back the original density matrix. Unlike the classical case, where the analogous situation refers to a weighted ensemble of phase-space points uniquely determined by the probability distribution, in the quantum situation, a mixed-state density matrix does not have a unique decomposition in terms of state vectors. Thus the ontology underlying the quantum master equation is substantially different from the classical situation (there can be many unravelings for a single quantum master equation).

It is therefore essential to distinguish between closed evolution, where the system state evolves without any coupling to the external world, *unconditioned open* evolution, where the system evolves coupled to an external environment but where no information regarding the sys-

tem is extracted from the environment, and *conditioned open* evolution where such information *is* extracted. This last aspect – system evolution *conditioned* on the measurement results via Bayesian inference – leads to an intrinsically nonlinear evolution for the system state, and distinguishes it from unconditioned evolution.

Quantum mechanics is intrinsically probabilistic, but classical theory is not. Since Newton's equations provide an excellent description of observed classical systems, including chaotic systems, it is crucial to establish how such a localized, or trajectory, description can arise quantum mechanically: the *strong* form of the QCT. However, in many situations, only a statistical description is possible even classically, and here we will demand only the agreement of quantum and classical distributions and the associated dynamical averages. This defines the *weak* form of the QCT and is the focus of the present paper. (An introductory review of these topics can be found in Ref. [12].)

While the specific nature of the interaction between subsystem and environment depends on the subsystem studied, the actual process of information extraction, and unavoidable coupling to other environmental channels, there do exist simple, yet physically significant general cases. The systems studied in this paper can be interpreted as undergoing a continuous position measurement [13], where either the results of measurement are not recorded, or all of the measurements in an ensemble are averaged over to erase the information regarding specific measurements. However, the entanglement between the position measuring readout and the subsystem will still produce a quantum backaction in momentum. In this unconditioned case, the subsystem is essentially an open system interacting with the meter through the coupling of its position states to the environment, without the localization due to conditioning. The form of this open system interaction, which falls into the class of Lindblad superoperators, rigidly separates the subsystem and its environment, and was formally studied in the literature of quantum open systems and quantum dynamical semigroups [14]. Phenomenologically, this interaction model is equivalent to the Caldeira-Leggett model of weak coupling to a high temperature environment, where damping effects can be neglected [15].

Although a classically chaotic system cannot approximate a closed quantum system via the traditional $\hbar \to 0$ route, there is good numerical evidence – at least for some systems – for the weak form of t0he QCT. Numerical studies of the Duffing oscillator and other systems have shown that the expectation values of a quantum system subject to an unconditioned continuous position measurement come into agreement with the expectation values of an (equivalent) open classical system, and that quantum phase space will come to capture certain classical phase space features [16]. In the case of the strong form of the QCT, studies have demonstrated the existence of nonzero Lyapunov exponents for conditioned systems, as well as inequalities which clearly delineate when the classical trajectory interpretation is valid in the conditioned case [17, 18].

An important distinction between the weak and strong forms of the QCT must be made. In the conditioned case, the master equation actively *localizes* the wavefunction about its expectation value, allowing *trajectory* level agreement between measured classical and quantum systems. However, in the unconditioned case, the inequalities governing the strong classical limit need not be satisfied and localization need not occur. The problem of understanding how classical and quantum systems begin to look like one another in a generic open system, even without the advantage of conditioning, has therefore remained open. As a final point, we note that while the strong form of the QCT must hold for all dynamical systems with a classical counterpart, it is not clear that a weak QCT must always exist outside the strong domain. The quantum delta-kicked rotor provides a good example of the failure of the weak QCT to exist in this sense [19]. The general problem of knowing in advance what governs this behavior is not yet resolved, although the work in this paper suggests that (effective) compactness of the accessible phase space plays an important role. Moreover, the violation of the conditions necessary to establish the strong form of the QCT need not prevent the existence of a weak QCT. Since the strong form of the QCT requires treating the localized limit, a cumulant expansion for the distribution function immediately suggests itself (Cf. [17]), whereas, for the more nonlocal issues relevant to the weak form of the QCT, a semiclassical analysis turns out to be natural, as will be demonstrated here in detail.

In this paper we investigate and discuss the underlying physical mechanisms responsible for the quantum-classical transition in an one-dimensional, open system with a bounded classically chaotic Hamiltonian, expanding on the themes of a shorter letter [20]. These arguments are topological in nature and should be generic for compact, one-dimensional hyperbolic regions, as well as for unbounded systems which stretch and fold in a manner analogous to bounded chaotic systems, unlike other studies which focus on calculations for a particular system of interest [21]. We show that, in this case, the classical limit is recovered via two parallel processes. First, environmental noise modifies chaotic classical phase space topology by terminating the production of small scale (late time) structures. This behavior has some parallels with recent numerical studies of a chaotic advection-diffusion problem with a periodic velocity field, as will be discussed later, though an exact correspondence between the two problems cannot be made at this time [22]. There, as here, the dynamics generates structure on increasingly smaller scales until diffusion terminates its development. Second, in the quantum picture, environmental noise acts as a *regulator*, attenuating nonlocal contributions to the semiclassical wavefunction, and, thereby, stabilizing a local semiclassical approximation from the pathologies which a classically chaotic system typically generates, so that it can now be associated with a noise-

modified (smoothed) classical phase space geometry. As a consequence of these processes, the local semiclassical approximation becomes stable at long times, allowing classical and quantum open systems to be brought into dynamical agreement at the level of *distribution functions*, rather than the *trajectory* level agreement one obtains from conditioning. The above arguments are very general and apply to a wide class of open systems. We demonstrate this agreement by employing the Wigner representation of the quantum density matrix and comparing it to the classical phase space distribution function. It has long been known that this approach has distinct mathematical and formal advantages [23]. Namely, it allows one to associate the accuracy of the semiclassical approximation with features of classical phase space geometry.

The key philosophy of this and other like-minded papers is that, for a classically chaotic system, correspondence and some notion of measurement or environmental coupling is inseparable. From the above considerations, we are able to derive conditions, involving $\hbar$, the strength of environmental coupling, and the long-time Lyapunov exponent describing the hyperbolic region of interest, which determine whether or not a semiclassical description is valid and, once these conditions are satisfied, a timescale beyond which the local semiclassical approximation becomes stable. We demonstrate this numerically for the Duffing oscillator in some detail and place it in the context of other numerical studies. We will begin, however, by reviewing the semiclassical and classical limits of closed nonlinear systems in the Wigner representation, and emphasize why they disagree with their associated classical distribution functions at short times and fail as $t \to \infty$. These points, while in the literature, have not always been explained in the context which this paper will later take for granted.

II. THE SEMICLASSICAL AND CLASSICAL LIMIT

The Wigner function, $f_W(q,p,t)$, is a phase space representation of the density matrix, $\hat{\rho}$, itself written in the position representation [24]. Along with the analogous classical phase space distribution function, $f_C(q,p,t)$, we will use it to compare the dynamics of open quantum and classical systems. Using the Wigner function as a tool for studying the quantum-classical transition is conceptually and practically advantageous. It allows one to compare classical and quantum dynamics in a somewhat similar representation (though there are pitfalls one must be aware of), rather than trying to compare very different objects such as, say, wavefunctions in $\mathbf{L}^2$ to classical trajectories. Additionally, the accuracy of semiclassical approximations can be directly linked to phase space geometry, making it easier to visualize the extent to which quantum and classical dynamical evolutions agree. For instance, the semiclassical Wigner distribution is more suited than the semiclassical wavefunction when dealing with classical turning points [23]. For a classically chaotic system, particularly one subject to observation, distribution functions give a clearer sense of global phase space topology, allowing one to examine the extent to which one is achieving dynamical agreement over the entire compact hyperbolic region of interest.

A. The Wigner Representation

The Wigner representation of an operator, $\hat{A}$, is defined as:

$$A_W(q,p,t) = \int_{-\infty}^{\infty} dX\ e^{-ipX/\hbar} \langle q + \frac{X}{2}|\hat{A}|q - \frac{X}{2}\rangle. \quad (1)$$

By this method one can associate any function of classical phase space variables, $A_C(q,p,t)$, with the Wigner representation of a Weyl ordered quantum operator by the prescription that the classical variables $q^n p^m$ are assigned to the Weyl ordered operator:

$$\frac{1}{2^n}\sum_{r=0}^{n}\binom{n}{r}\hat{q}^{n-r}\hat{p}^m\hat{q}^r. \quad (2)$$

The Wigner function is the Wigner representation of the general mixed state density operator $\hat{\rho} = \sum_i c_i|\psi_i\rangle\langle\psi_i|$ yielding

$$\begin{aligned} f_w(q,p,t) \ &= \ \frac{1}{2\pi\hbar}\int_{-\infty}^{\infty} dX \exp\left(\frac{-ipX}{\hbar}\right) \times \\ &\sum_i c_i\psi_i(q+\frac{X}{2},t)\psi_i^*(q-\frac{X}{2},t). \end{aligned} \quad (3)$$

Following this method one can show that the Wigner function reproduces the ensemble average of any Weyl ordered operator. That is:

$$\begin{aligned} \langle\hat{A}\rangle \ &= \mathrm{Tr}(\hat{A}\hat{\rho}) \\ &= \int_{-\infty}^{\infty} dq \int_{-\infty}^{\infty} dp\ A_W(q,p,t) f_W(q,p,t). \end{aligned} \quad (4)$$

In other words, there is a correspondence between any *classically* observed function of phase space variables and a quantum observable. The opposite is not true, since there is no specific classical analog to, say, $\hat{p}\hat{q}\hat{p}$. However, if one is investigating the degree to which quantum dynamics approximately reproduces classical dynamics – since quantum mechanics is the correct theory and classical mechanics is only an approximation – the ability to establish a correspondence between any classical quantity and a quantum operator is sufficient.

Unlike a classical phase space distribution function, the Wigner function is only a quasiprobability distribution, as it can take on negative values due to nonlocal quantum interference effects, thereby violating the mutual independence of different outcomes. This condition also implies that the Wigner function cannot generally be used

as a conditional probability distribution. It also leads to upper and lower bounds on the Wigner function of $\pm(\pi\hbar)^{-1}$, which prevents it from being a delta function, like a classical trajectory, at finite $\hbar$ [25]. As a consequence it should not be confused with a phase space distribution function which is a true positive definite probability distribution capable of recording averages over arbitrarily small phase space regions. The degree to which a Wigner function can capture a local average depends on the degree to which the region being integrated over is receiving strong quantum interference effects from locations outside of the integrated region. Certainly if the region is smaller than $2\pi\hbar$ this will be the case. The suggestive similarities between the two functions, therefore, needs to be tempered somewhat by their substantial differences.

The equation of motion for the Wigner function is given by the Wigner representation of the equation of motion for the density operator:

$$\frac{\partial f_W}{\partial t} = \hat{L}_C f_W + \hat{L}_Q f_W, \tag{5}$$

where the classical Liouville operator

$$\hat{L}_C \equiv -p\partial_x + \frac{\partial V}{\partial x}\partial_p \tag{6}$$

and the quantum operator

$$\hat{L}_Q \equiv \sum_{n\geq 1} \frac{\hbar^{2n}(-1)^n}{(2^{2n}(2n+1)!)} \partial_x^{2n+1} V \partial_p^{2n+1}. \tag{7}$$

The form of this evolution equation again suggests an intuitive, but misleading interpretation [26]. In the equation of motion, $\hbar$ only appears in the $\hat{L}_q$ term. So it is tempting to suggest that, as $\hbar \to 0$, the "quantum contributions" to the evolution of the Wigner function likewise decrease. However, all of the momentum derivative terms in both $\hat{L}_Q$ and $\hat{L}_C$ are proportional to $\hbar^{2n}\partial_p^{2n+1} f_W$. Since, by definition,

$$f_W \sim \exp\left(\frac{ipX}{\hbar}\right), \tag{8}$$

after one takes the appropriate momentum derivatives, it is clear that, like the wavefunction, f_W is $O(\hbar^{-1})$ to leading order in $\hbar$. This is a manifestation of the singular nature of the $\hbar \to 0$ limit. One can never expect quantum corrections to smoothly disappear as $\hbar$ is decreased due to this essential singularity. We will address the topological importance of this singularity for chaotic systems later, but it is worth mentioning again, as in the Introduction, that it is important even for simple systems such as the harmonic oscillator and free particle distributions. These are the rare cases where symplectic and unitary symmetry are not at odds in the dynamics (since $L_Q = 0$). Nevertheless, when computing eigenfunctions or in the semiclassical approximation, their Wigner representation will produce increasingly rapid oscillations as $\hbar \to 0$ and will not tend to a positive distribution. To eliminate the rapid oscillations, one often introduces an ad hoc filter, as in the case for the Husimi-type Gaussian filters [27, 28]. This can forcibly produce positive-definite distributions but has no underlying dynamical justification.

Another common misconception is connected to the role of unitarity in the Wigner evolution [19]. Clearly, since quantum mechanics is unitary, the full quantum Liouville operator, $\hat{L}_Q + \hat{L}_C$ generates a unitary evolution for the Wigner function. Similarly, if one is only left with $\hat{L}_C$, one has the usual classical symplectic Liouville evolution. It is therefore enticing to think of $\hat{L}_Q$ as some sort of unitary correction or deviation from a symplectic symmetry. One could then try to think of this term as being solely responsible for generating quantum interference [29]. However, as the previous paragraph suggests, and has been discussed in Ref. [19], the roles of $\hat{L}_C$ and $\hat{L}_Q$ cannot be so neatly divided. The basic point to note is that the classical Liouville evolution for nonlinear potentials takes initial Wigner functions into phase space functions that cannot be associated with density matrices [19]; thus this evolution is not positive in the quantum sense (it violates quantum unitarity by failing to maintain the positive semi-definiteness of the initial density matrix). Therefore, $\hat{L}_Q$ is not a purely unitary operator either; it must possess a non-unitary piece to precisely cancel off the offending non-positive classical contribution which has nothing to do with (nonlocal) quantum interference.

Note that while the classical Liouville operator cannot generate negative regions for a *classical* positive-definite distribution function by itself, it will propagate interference and negativity for a *quantum* Wigner distribution which is generically not positive-definite (the only pure-state Wigner function which is positive over phase space is the Gaussian [30]). This is again clear for the harmonic oscillator where the quantum and classical evolutions are identical. However, since $\hat{L}_C$ is purely local, it cannot generate nonlocal interference terms which are a hallmark of quantum evolution [31].

B. The Semiclassical Limit

The semiclassical wavefunction is the singular and constant part of a general wavefunction in the $\hbar \to 0$ limit. In the textbook presentation, the phase of the quantum wavefunction is represented as a power series in $\hbar$ [32]. As $\hbar$ decreases, terms of $O(\hbar)$ and higher vanish and one is left with terms of order $\hbar^0$ and $\hbar^{-1}$. The non-vanishing terms make up the semiclassical wavefunction, the leading order term being responsible for the previously mentioned $\hbar = 0$ essential singularity. In this sense, any small $\hbar$ view of the classical limit must focus on the semiclassical regime since the semiclassical wavefunction *is* the irreducible part of the wavefunction in this limit. The standard presentation tends to view this process as sim-

ply representing the two lowest order terms in a perturbation series for the phase of the wavefunction. However, the higher order terms in this series, in addition to being notoriously difficult to calculate, are rarely useful. The remaining terms can be thought of as a vanishing, $O(\hbar)$ error, and not as a series of higher order terms waiting to be explicitly calculated [33].

Most importantly, the semiclassical wavefunction can be directly associated with the evolution of classical phase space curves. The formal procedure constructs an initial wavefunction from an N-dimensional Lagrangian manifold embedded in a $2N$-dimensional phase space [33]. In this paper, phase space is two dimensional and so the associated Lagrangian manifold studied is a curve. An initial wavefunction is chosen of the form:

$$\psi(q,0) = A_0(q)\exp\left[\frac{i}{\hbar}S_0(q)\right] \tag{9}$$

where $A_0(q)$ and $S_0(q)$ are real-valued functions and $|A_0(q)|^2 = 1$. This form naturally induces a Lagrangian curve in phase space, if the associated momentum has a well-defined classical limit. Namely,

$$\lim_{\hbar\to 0} i\hbar\frac{\partial}{\partial q}\psi(q,0) = A_0(q)\frac{\partial S_0(q)}{\partial q} \equiv p(q). \tag{10}$$

The evolution of the curves can be described via an analogy with action-angle coordinates for integrable systems. It is possible to choose a canonical coordinate Q on the curve such that the points along the curve are distributed uniformly in Q. The coordinate Q will then become a new canonical variable with a conjugate momentum P. The original coordinates (q,p) are related to (Q,P) by the action, $S_0(q,P)$, defined by the initial conditions. If the system is integrable the (Q,P) will be the angle and action respectively, as the angle variables are uniformly distributed along invariant tori. The action must then satisfy:

$$Q = \frac{\partial}{\partial P}S_0(q,P), \tag{11}$$

in addition to defining the usual momentum by its gradient with respect to q. Likewise, the amplitude of the initial wavefunction can be defined in terms of this action. The probability density of the wavefunction is proportional to the density of points on the curve at q

$$|\psi_0|^2 = A^2\left|\frac{\partial Q}{\partial q}\right| = A^2\left|\frac{\partial^2 S_0}{\partial q\partial P}\right|, \tag{12}$$

where A is a positive, real constant. In N-dimensions this would be a full Jacobian determinant. The initial amplitude of the semiclassical wavefunction is therefore given by

$$A(q) = A\left|\frac{\partial^2 S_0}{\partial q\partial P}\right|^{1/2}. \tag{13}$$

By first defining the action at time t for the j-th path as

$$\begin{aligned} S_j(q,t,P) &= S_0(q_{0j}) + \int_{q_{0j}}^{q} dq' p_j(q',t,P) \\ &\quad - \int_0^t dt' H(q_{0j}, p_{0j}(q_{0j},t',P),t'), \end{aligned} \tag{14}$$

the semiclassical wavefunction is given by:

$$\begin{aligned} \psi(q,t) &= \sum_{j=1}^{N} A_j(q,t)\exp\left(\frac{i}{\hbar}S_j(q,t,P) - \frac{i\pi}{2}\nu_j\right) \\ &\quad + O(\hbar), \end{aligned} \tag{15}$$

where ν_j is the j-th Morse index, defined as the number of times the determinant is equal to zero along the path connecting (q_{0j},p_{0j}) to (q,p_j), and the amplitude of the j-th branch is

$$A_j(q,t) \equiv \left|\frac{\partial^2 S_j}{\partial q\partial P}\right|^{1/2}, \tag{16}$$

as shown in Ref. [23].

By substituting the semiclassical wavefunction into the definition of the Wigner function, one can construct a geometric interpretation of the accuracy of a semiclassical analysis. For the purpose of clarity, we will assume we are dealing with a pure state density matrix, the extension to mixed states being straightforward. The semiclassical Wigner function then becomes:

$$\begin{aligned} f_w(q,p,t) &= \frac{1}{2\pi\hbar}\int_{-\infty}^{\infty} dX \sum_{ij}\mathcal{A}_{ij}\exp\left[\frac{i}{\hbar}(S_i(q+X/2,t)\right. \\ &\left. -S_j(q-X/2,t) - pX) - \frac{i\pi}{2}(\nu_i-\nu_j)\right], \end{aligned} \tag{17}$$

where $\mathcal{A}_{ij} \equiv A_i(q+X/2,t)A_j(q-X/2,t)$ and the (Q,P)-dependence has been dropped for clarity.

To get a sense of the primary contributions to this integral as $\hbar$ is brought to zero and the integrand rapidly oscillates, we examine the stationary phase condition:

$$\frac{d}{dX}(S_i(q+X/2,t) - S_j(q-X/2,t) - pX) = 0. \tag{18}$$

In the stationary phase approximation, the Wigner function is separated into a singular stationary part and an additional $O(\hbar^{1/2})$ oscillatory part [34]. Therefore, the stationary phases are the most relevant contributions in the $\hbar\to 0$ limit, as rapid oscillations become less significant. After substituting the expression for the evolved action, the stationary phase condition becomes:

$$\frac{1}{2}(p_i(q+X/2,t) + p_j(q-X/2,t)) = p(q,t). \tag{19}$$

If $i=j$ we get the famous Berry midpoint rule: $\frac{1}{2}(p_i(q+X/2)+p_j(q-X/2)) = p(q,t)$ [23]. That is, the stationary

phase contributions at a point (q,p) come from the average of the momenta on a given solution curve evaluated at the end of an interval of width X about q. If $i \neq j$, then the contributions come from the average momenta from two different solution curves. The stationary phases are then given by the area between the solution curves and the chord which solves the midpoint rule.

One problem is that, if the point (q,p) is particularly close to a curve, $p_i(q)$, then the stationary phase points will coalesce, invalidating the stationary phase method. Likewise, the WKB wavefunction itself is not valid near turning points, as the Jacobian vanishes. However, these cases can be remedied by using the uniform approximation, which yields a symmetric Airy function, rather than sinusoidal, behavior [35]. The uniformized Wigner function is valid both near turning points and near the curve itself, so these cases do not invalidate the general semiclassical approach. Therefore, if (q,p) is too close to a given branch, the expression for the semiclassical contribution for that branch should be replaced by the uniformized form. The only remaining problem which can invalidate the validity of the expression is the appearance of catastrophes when (q,p) is a focal point of a curve. These can be dealt with analytically but these methods, also studied by Berry, are outside the realm of this paper.

Close to the classical curve $p_i(q)$, the uniformized WKB approximation for the Wigner function has an Airy "head" of width $\sim \hbar^{2/3}$ and peak height $\sim \hbar^{-2/3}$. In this limiting case, the uniform approximation can be further simplified and written in the form of a "transitional approximation" which is valid only very near $p_i(q)$. Remarkably, the $\hbar \to 0$ limit of the transitional approximation is indeed a classical delta function, which allows the Wigner function picture to give a physically clearer presentation of the classical limit than others.

The above progression gives rise to the intuition that if the interference fringes can be suppressed, quantum Wigner functions and classical distributions may converge, and that they then can collectively be brought to a classical curve as $\hbar \to 0$. In order for this to happen, some points need to be considered. First, the semiclassical quantum Wigner function will go through three distinct phases in its evolution, if the underlying classical dynamics is chaotic, as laid out by Heller and Tomsovic in Ref. [6]. During the first phase, if the initial condition used is that of a classical distribution, there will be little disagreement between the quantum and classical evolutions. This phase is only valid when the "area-$\hbar$" rule holds, i.e., the stationary phase area is greater than $\hbar$, and the timescale at which this fails to be the case is logarithmic. When this rule becomes commonly broken, the semiclassical construction will no longer reproduce classical dynamics. This is the second phase, where the semiclassical approximation reproduces the wave function dynamics, but is distinctly nonclassical. At a longer timescale, proportional to inverse powers of $\hbar$, the semiclassical approximation fails, as the distance between classical manifolds becomes so close that the cumulative interference cannot be locally ascribed to any given curve. So, in the first, classical regime, there is little interference. In the second, semiclassical regime there is some, possibly strong, quantum interference, but it is in the form of local fringing about classical curves. In the final, fully quantum phase, there is strong global interference, and local classical manifold evolution is no longer of much relevance to a quantum picture.

In order to maintain a stable classical limit, it must be possible to keep a system in the first, classical regime, which is the goal of the QCT and is impossible for closed classically chaotic systems. This imposes a smoothness condition on the underlying classical geometry for a transition to occur. Second, there are two sources of interference: local Airy "shadows" of the short wave curve and nonlocal contributions from multiple curves. The nonlocal source of interference is clearly more problematic if we wish a weak QCT to hold and must be filtered somehow; we show how this happens below in open systems, via the same physical process generated by an unconditioned environment that simultaneously smoothes the classical phase space geometry.

III. OPEN SYSTEMS AND MEASUREMENT

To model the interaction between a subsystem and its measuring device we choose the form of an unconditioned continuous position measurement. This provides the minimum level of interaction necessary to bring quantum and classically chaotic dynamical systems into agreement with one another at the level of distribution functions. The model of a conditioned continuous position measurement (i.e., evolution of the system density matrix taking the results of measurement into account) is given by the following master equation:

$$\begin{aligned} d\rho &= -\frac{i}{\hbar}[H,\rho] + k[X[X,\rho]]dt \\ &\quad -\frac{\sqrt{k}}{2}([X,\rho]_+ - 2\rho\langle X\rangle)dW, \end{aligned} \tag{20}$$

where the observed measurement record is given by

$$dy = \langle X\rangle dt + \frac{1}{\bar{k}}dW. \tag{21}$$

In the above equation $\langle X\rangle = Tr(\rho X)$, dW is the Wiener measure $[(dW)^2 = dt]$, k measures the strength of the interaction between the subsystem and the measuring apparatus and $\bar{k}$ measures the rate at which information about the system is being extracted. The fractional measure of extracted information is given by the efficiency of the measurement $\eta \equiv \bar{k}/8k$. The first term is just the unitary evolution for the closed system, the second is a diffusive term arising from quantum backaction, and the third represents the conditioning due to the measurement.

The conditioned evolution can localize the state about the measured position value; the extent of this localization (increasing $\bar{k}$) must however be tempered by the associated increase of backaction noise (concomitant increase in k). Nevertheless, inequalities can be derived that show under what conditions both of these conflicting effects can be reconciled and agreement between classical and quantum dynamics achieved at the level of trajectories [17, 18] – the strong form of the QCT.

If one averages over all obtained measurement records, one obtains the master equation for an unconditioned evolution:

$$d\rho = -\frac{i}{\hbar}[H,\rho] + k[X[X,\rho]]dt. \tag{22}$$

This evolution can also be achieved by setting the efficiency of the measurement, and, therefore, $\bar{k} = 0$. Once one does so, the localization inequalities which characterize the strong form of the QCT fail, showing the inability of the weak QCT to capture trajectory level chaos and the need for the distribution function approach employed here. The evolution equation is the same as that for a the Caldeira-Leggett model in the weak coupling, high temperature approximation [15]. The key point here is that while the conditioning term is absent, the backaction term remains. This is very different from the classical case, where averaging over measurements simply gives back the closed-system Liouville equation, thus highlighting the contrast between the active nature of quantum measurements versus the passive nature of classical measurements.

The master equation (22) is the starting point in our analysis of the weak QCT utilizing the Wigner function. In the Wigner representation, this equation becomes

$$\frac{\partial f_W}{\partial t} = \hat{L}_C f_W + \hat{L}_Q f_W + D\frac{\partial^2 f_w}{\partial p^2}, \tag{23}$$

where the diffusion coefficient $D = \hbar^2 k$. If we set $\hat{L}_Q = 0$, we obtain a dual classical evolution equation, which, given its form, we will call the dual Fokker-Planck equation. Note that this Fokker-Planck equation does *not* represent the dynamics of an associated classical observed system. Here it has two key roles: it represents the classical template for a semiclassical open-system analysis and also the proper (approximate) classical limiting form if the weak QCT were to hold. This particular Fokker-Planck equation is better viewed as simply a classical dual of the quantum master equation (23), without an independent physical existence.

IV. MODIFICATION OF PHASE SPACE GEOMETRY FOR A CHAOTIC SUBSYSTEM

The first step in our analysis is the study of the dual Fokker-Planck equation. As earlier mentioned, following a semiclassical line of reasoning, the motivation for this is that the measurement/environmental interaction modifies the geometry of a chaotic classical phase space in a manner which can allow dynamical agreement between classical and quantum systems. The key point is that, due to the diffusion term, one necessarily sees a termination in the level at which one can discern the long-time development of fine structure. The (exponential) long-time development of structure is a hallmark of classically chaotic systems in a compact space, and, as discussed in the previous section, leads to disagreement between classical and semiclassical results, followed by a complete failure of semiclassical analysis. But, as these structures are averaged over, the resulting smoother phase space geometry can be consistent with the existence of a local semiclassical description. We will show below that the diffusion term in the Fokker-Planck equation terminates the development of small scale structures at a finite time, denoted by t^*. At this time, there will be an associated area, $l(t^*)^2$, below which no smaller phase space structures can be discerned.

To understand the termination of structure, we consider the Langevin equations underlying the dual Fokker-Planck equation. These are given by

$$dq = pdt/m \tag{24}$$

and

$$dp = f(q)dt + \sqrt{2D}dW, \tag{25}$$

where $f(q) = -\partial V(q)/\partial q$, dW is the Wiener measure $[(dW)^2 = dt]$, and D is the noise strength. Since D is constant, one can consistently write $dW = \xi(t)dt$, where $\xi(t)$ is a rapidly fluctuating force satisfying $\langle\xi(t)\rangle = 0$ and $\langle\xi(t)\xi(t')\rangle = \delta(t-t')$ over noise averages.

A hyperbolic region of the phase space of a bounded chaotic Hamiltonian system is foliated by its unstable manifold, which emerges from the stretching and folding behavior induced when nonperiodic solution curves are confined to a bounded region. A trajectory in the neighborhood of a hyperbolic fixed point will create large scale structures, due to its exponential growth away from the hyperbolic point. As it evolves, since it can only explore the energetically allowed region, it will fold onto itself and create smaller scale structures. For a bounded chaotic region, the curve will eventually fill the allowed space. The important consequence for this analysis is that this filling is done preferentially. Large scale structures are initially generated by rapid stretching and are associated with short time scales. The smaller scale fine structures are then filled in afterwards as the system continues to fold on itself and are, therefore, a late time feature.

To see how environmental noise modifies this picture, we perform a perturbative expansion of the solution curve in the small noise limit in the neighborhood of a hyperbolic fixed point $(q_{eq}, 0)$, where $f(q_{eq}) = 0$, where $\sqrt{2D}$ is treated as the small noise parameter [36, 37]. This assumption is physically justified by the argument that the affected noise scale in phase space should be smaller than

that of the system dynamics, and this is checked in later simulations for purposes of self consistency. As discussed in the introduction, the premise of these sort of open system analyses is that the system is interacting weakly with its environment. After all, a measurement is not supposed to be so large in strength that it strongly alters the system dynamics. This implies a separation between systematics and environmental effects which makes a perturbative approach natural. To leading order in $\sqrt{2D}$, we can therefore separate the dominant systematic components from the noisy components via $q(t) \approx q_C(t) + q_N(t)$ and $p(t) \approx p_C(t) + p_N(t)$, leading to the usual Hamilton's equations for q_C and p_C, and to the coupled equations $dq_N = p_N dt/m$ and $dp_N = m\lambda^2 q_N dt + dW$, where $m\lambda^2 = \partial f(q_{eq})/\partial q$ defines the local Lyapunov exponent, λ. These have the solution,

$$\begin{aligned} q(t) &= q_{eq} + C_+ e^{\lambda t} + C_- e^{-\lambda t} \\ &\quad + \frac{\sqrt{2D}}{2m\lambda} \int_0^t du \xi(u) \left(e^{\lambda(t-u)} - e^{-\lambda(t-u)} \right), \end{aligned} \tag{26}$$

with an analogous expression for $p(t)$. To see the effect of this on the foliation of the unstable manifold, one needs to transform from the position and momentum basis into the stable and unstable directions. The dimensional scalings $q' = \sqrt{\lambda m} q$ and $p' = p/\sqrt{\lambda m}$ are introduced so that the rescaled position and momentum have the same dimensions and also so that the stable and unstable directions are orthogonal. An arbitrary time rescaling, which would give the correct units, would not guarantee orthogonality.

If we project the solutions for $q' = \sqrt{\lambda m} q$ and $p' = p/\sqrt{\lambda m}$ along the stable (-) and unstable (+) directions, we find the following expression for the components of the noisy trajectories evolution in these two directions:

$$\begin{aligned} u_\pm(t) &= \frac{1}{\sqrt{2}}(q' \pm p') \\ &= \sqrt{2\lambda m} C_\pm e^{\pm\lambda t} \pm \sqrt{\frac{D}{\lambda m}} \int_0^t du \xi(u) e^{\pm\lambda(t-u)}, \end{aligned} \tag{27}$$

One can now analyze the effects of these noisy trajectories on the evolution of the distribution function which they unravel. The average over all noisy realizations of the displacement in the stable and unstable directions is given by $\langle u_\pm \rangle = \sqrt{2\lambda m} C_\pm e^{\pm\lambda t}$, as expected from a perturbation in the neighborhood of a hyperbolic fixed point. More information is found in the second order cumulants. Whereas, the stable and unstable directions have variances of $\pm\frac{D}{2m\lambda^2}(e^{\pm 2\lambda t} - 1)$, the off-diagonal cumulant is $\langle u_+ u_- \rangle - \langle u_+ \rangle \langle u_- \rangle = -Dt/(m\lambda)$, displaying the sort of linear spreading associated with a Wiener process. In forward time, where the evolution of a trajectory is determined by the unfolding of the unstable manifold, this spreading indicates that, as the trajectory evolves, it will simultaneously smooth over a transverse width in phase space of size

$$\sqrt{Dt/(m\lambda)}. \tag{28}$$

One is left with a picture of a curve following a classical path in the unstable direction while carrying small amounts of transverse noise. In a bounded, compact phase space region, this implies a termination in one's ability to measure the position and momentum of the trajectory on a scale smaller than the aforementioned width. In other words, the fine structures associated with a chaotic region will be smoothed over in the averaging process, causing the development of large scale structures which occur prior to this termination time to become pronounced. Given a set of parameters associated with this compact phase space region, one can estimate the value and scaling associated with this termination time, t^*.

Consider an initially small compact region of phase space area u_0^2, then its current phase space "length" will be approximately $u_0 e^{\bar{\lambda} t}$, where $\bar{\lambda}$ is the time-averaged positive Lyapunov exponent. If the trajectory is bounded within a phase space area A, this implies that the typical distance between neighboring folds of the trajectory will be given by

$$l(t) \approx A/(u_0 e^{\bar{\lambda} t}). \tag{29}$$

This formula is, of course, only valid at long time scales after which the curve has begun to fold on itself. Since this is a classical phase space, u_0 can be chosen to be arbitrarily small, so one must be careful that enough time for folding to occur has passed before utilizing the above equation. One can, in this spirit, estimate a "folding time" and compare it with t^* to again insure that this analysis is self-consistent. This is typically a rapid time scale, but in any case, one cannot make u_0^2 as small as possible since it has a minimum size set by the quantum uncertainty principle, when its is eventually compared to a quantum distribution to explore the QCT. Note also, that the length of a long time scale is also implied by the appearance of the time-averaged Lyapunov exponent, $\bar{\lambda}$.

Since phase structures can only be known to within the width specified by the noisy dynamics, there will come a time at which the scale $l(t)$ set by this folding will be smaller than the scale at which lengths are averaged over Eqn. (28). The time at which any new structures will be smoothed over is therefore defined by

$$l(t^*) \approx \sqrt{Dt^*/(m\bar{\lambda})}. \tag{30}$$

After this time, no new structures will be discerned, since they will be smaller than the averaging scale set by the noisy dynamics. This implies the existence of a phase space area $l(t^*)^2$ below which phase space structures are smoothed over.

The dual Fokker-Planck equation for a chaotic system is such that we can only discern large scale structures (small and large being relative to the cutoff $l(t^*)$ produced prior to t^*). When constructing a classical limit for the open quantum evolution (23), we now only have to capture these larger, short-time dynamical features and not the full chaotic evolution of the classical Liouville equation with its – from a quantum perspective – small-scale pathologies.

Before preceding, we wish to mention a somewhat analogous situation which occurs in studies of chaotic advection-diffusion in fluid dynamics. The evolution equation for the concentration density, $c(\mathbf{x},t)$, of a set of particles diffusing in a fluid without sinks or sources is given by

$$\frac{\partial c}{\partial t} + \nabla c \cdot \mathbf{v} = \kappa \nabla^2 c, \tag{31}$$

where $\mathbf{v}(\mathbf{x},t)$ is the velocity field of the tracer particles. This matches the classical Fokker-Planck equation studied here, if one sets

$$\mathbf{v} = \left(\frac{p}{m}, -\frac{\partial V}{\partial q}\right) \tag{32}$$

and the gradient is taken with respect to q and p. Diffusion, in our case, is only with respect to p. The phase space distribution function is then regarded as the concentration of particles in phase space in a given region, which is certainly an appropriate interpretation.

A numerical analysis performed in Ref. [22] showed results similar to our predictions where, for a certain vale of κ, equivalent to D in our case, the evolution converged to a stationary pattern at a finite time, with only residual diffusion afterwards. The final pattern was termed an inertial manifold and related to the unstable manifold. Moreover, the authors of Ref. [38] were able to analytically show the existence of such a manifold beyond a critical κ value. This seemed to imply that the qualitively correct classical analysis provided here could perhaps be made more rigorous by their method. However, their analysis relied significantly on applying periodic boundary conditions to the concentration evolution and the gaps the spectrum of the Laplacian they create. As a result, their techniques have not been applied to our open boundary situation. Though we tried using the fact that our phase region is bounded to imply approximately similar boundary conditions, no such analysis was successful. Still, there are qualitative similarities and the two fields may well mutually inform each other in the future. Of course, this is a purely classical analysis and does not bear directly on the quantum evolution, though it does so implicitly since the semiclassical evolution tracks the classical manifold structure.

V. SEMICLASSICAL ANALYSIS FOR AN OPEN CHAOTIC SYSTEM

We now turn to the semiclassical analysis of the open system master equation (23) in order to estimate the conditions under which a weak QCT might exist. We begin by rewriting the semiclassical Wigner function in the weak noise limit utilized in the previous section. In this limit, the classical action is modified to $S(q,t) \approx S(q_C,t) - \sqrt{2D}\int_0^t dt\xi(t)q_C(t)$, as in Ref. [39]. The first term will evolve classically, as discussed in Section III, as will the position coordinate which appears in the second term. If we insert the above semiclassical action into the expression for the Wigner function we get the following result:

$$\begin{aligned} f_W(q,p,t) \;=\; & \int dX\; \frac{e^{-ipX/\hbar}}{2\pi\hbar} \sum_{i,j}^{N} \mathcal{A}_{ij} \\ & \exp\left(-\frac{i}{\hbar} X\sqrt{2D}\int_0^t dt'\; \xi(t')\right) \times \\ & \exp\left(\frac{i}{\hbar}(S_{Ci}(q_{C+},t,P) - S_{Cj}(q_{C-},t,P)) \right. \\ & \left. -\frac{i\pi}{2}(\nu_i - \nu_j)\right), \end{aligned} \tag{33}$$

noting that, since the amplitude is a second derivative and the noisy perturbation is linear, noise only effects the action to lowest order. If we next average over all noisy realizations, the following suggestive expression for the noise averaged semiclassical Wigner function is obtained:

$$\begin{aligned} & \int dX\; \frac{e^{-ipX/\hbar}}{2\pi\hbar} \exp\left(-\frac{Dt}{\hbar^2}X^2\right) \sum_{i,j}^{N} \mathcal{A}_{ij} \times \\ & \exp\left(\frac{i}{\hbar}(S_{Ci}(q_{C+},t,P) - S_{Cj}(q_{C-},t,P)) \right. \\ & \left. -\frac{i\pi}{2}(\nu_i - \nu_j)\right). \end{aligned} \tag{34}$$

The only alteration to the expression for the semiclassical wavefuntion to lowest order in the noise strength is the appearance of a new Gaussian term.

The presence of noise acts as a dynamical low-pass Gaussian filter of semiclassical phases, attenuating large X contributions. For any solutions to the above equation, phases will be suppressed which have wavelengths greater than

$$X \approx \hbar/\sqrt{2Dt}. \tag{35}$$

These are the long, nonlocal "De Broglie" wavelength contributions to the semiclassical integral, the very sort of contributions previously identified as being particularly problematic in terms of obtaining a weak QCT. The filter prevents the integral from becoming overwhelmed by long range contributions as stretching and folding occurs which can lead to disagreement with classical results, as well as the eventual failure of the approximation.

If we combined the above with the classical result from the last section we can see the combined effect of our open system analysis. The diffusion causes two effects: suppression of nonlocal phases in the semiclassical integral beyond a certain scale given by Eqn. (35) and a smoothing of the dual classical phase space over fine structures smaller then a scale given by Eqn. (30).

Each of these effects overcomes the two semiclassically identified difficulties associated with a weak QCT for chaotic systems: the Wigner function is no longer dominated by nonlocal contributions and also does not need to

track, nor does it receive interference from, very fine scale structures. From these two scales we should, therefore, be able to set a (semiclassical) criteria for the existence of a weak QCT for a bounded one-dimensional chaotic system. Physically, the local semiclassical approximation is valid when the primary contributions to the semiclassical integral at a given point (q, p) come from the local branch of the trajectory on which the point is located. This will occur only when the scale at which local classical smoothing occurs matches or exceeds the filtering scale for semiclassical phases. When this occurs the nearest possible branch which is capable of delivering nonlocal interference effects will have those effects filtered within the semiclassical integral. As a result one can recover the usual short wave semiclassical picture of a trajectory "decorated" only by local interference fringes.

More specifically, if we rescale the filtering condition (35) and set it equal to the smoothing scale from the dual classical evolution, we obtain the following semiclassical criteria for the weak QCT:

$$\frac{\sqrt{\bar{\lambda}m\hbar}}{\sqrt{2Dt^*}} \lesssim l(t^*). \tag{36}$$

One should recall that t^* – the time at which the production of fine structures is terminated – is an entirely classically determined quantity, as defined by Eqn. (30) in the previous section. Using Eqn. (30) one can rewrite Eqn. (36) as:

$$\sqrt{2}Dt^* \gtrsim \bar{\lambda}m\hbar. \tag{37}$$

Note that, if this inequality is satisfied, t^* can then also be interpreted as the time scale beyond which a semiclassical approximation becomes stable for an open quantum system. After this time, classical dynamics should approximate quantum dynamics sufficiently. An interesting physical interpretation is more apparent on rewriting the inequality as $l(t^*)^2 \gtrsim \hbar$, where l^2 is an areal scale in phase space for the diffusion-averaged dual classical dynamics. It has the dimension of a classical action and, as such, Eqn. (37) is a statement of the validity of the associated semiclassical approximation.

VI. NUMERICAL SIMULATIONS

The analysis in the preceding sections has helped to establish a set of criteria which, once met, allow the existence of a weak QCT for classically chaotic systems. Given their somewhat heuristic nature, it is important to examine these predictions numerically. In the quantum evolution, once the inequalities are satisfied, noise will filter nonlocal quantum interference between the surviving large scale phase space structures, so large scale coherences should not be present. If not, one will essentially see a global phase space diffraction pattern, with large-scale coherences persisting between all parts of the bounded phase space region, as in Figure 1.

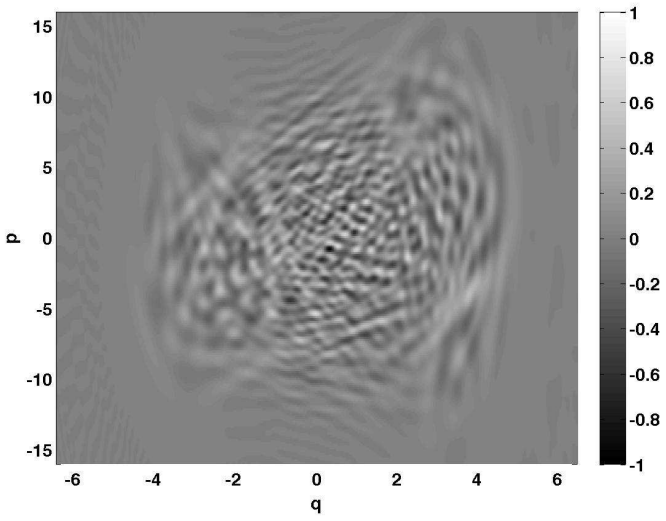

FIG. 1: Phase space rendering of the Wigner function for the Duffing system at time $t = 314$ periods of driving. The nonlocal interference is significant and cannot be associated with specific classical structures. This plot is taken at a relatively small D value (10^{-4}) for resolution purposes. The value of $\hbar$ is set equal to 1 in order to clearly demonstrate this effect.

The most direct numerical test is the close examination of the time evolution of both the classical and quantum distribution functions for the quantum and dual classical evolutions. In this manner one can examine whether, at the D values given by the inequalities and for times greater than t^*, the expected phase space features are present for the template classical distributions and quantum Wigner functions. Such a direct examination is necessary as other, seemingly logical measures, can sometimes be misleading. For instance, looking at expectation values is not always helpful, as numerical simulations of chaotic systems have failed to find well-defined break times and expectation values can agree well for surprisingly long time scales and accuracy even without the presence of environmental noise [6]. Other measures, such as suppression of the integrated negativity of the Wigner function, also are not necessarily signatures of quantum-classical correspondence, as shown in Ref. [19].

Numerical solutions of the quantum master equation (23) for the Wigner function and of the corresponding dual classical Fokker-Planck equation were carried out using a split operator spectral method implemented on parallel supercomputers [40]. Suppose the time evolution of a function, $f(t)$, satisfies the operator equation:

$$\frac{\partial f}{\partial t} = (\hat{L}_A + \hat{L}_B)f. \tag{38}$$

where the separate evolutions given by $\hat{L}_A$ and $\hat{L}_B$ can be implemented exactly. The exact solution to this equation is given by:

$$f(t) = e^{((\hat{L}_A+\hat{L}_B)t)}f(0). \tag{39}$$

Since $\hat{L}_A$ and $\hat{L}_B$ do not commute in general, the fact that the individual evolutions are known exactly is not of direct use. An integration scheme for a small timestep Δt can be constructed simply, however, using the Campbell-Baker-Hausdorff theorem:

$$f(\Delta t) \approx e^{(\frac{\Delta t}{2}\hat{L}_A)} e^{(\Delta t \hat{L}_B)} e^{(\frac{\Delta t}{2}\hat{L}_A)} f(0) + O(\Delta t^3). \quad (40)$$

With the assumption that the exponentiated operators can be applied exactly, this method is accurate to second order in Δt. The third order correction term is

$$\frac{1}{24}(\Delta t)^3 [\hat{L}_A + 2\hat{L}_B, [\hat{L}_A, \hat{L}_B]] f(0), \quad (41)$$

which can be evaluated to show the accuracy of the approximation. One can then find the solution of these function to a desired accuracy at a time $t = N\Delta t$.

In the present case, the evolution operator is $\hat{L}_{cl} + \hat{L}_q + D\partial_p^2$ for the Wigner evolution and is the same, but with $\hat{L}_q = 0$ for the dual classical evolution. We split this into three operators, the "stream" operator $-(p/m)\partial_q$, the "kick" operator proportional to potential derivatives, which differs for the classical and quantum cases, and the momentum diffusion operator. As each piece involves either derivatives of position or momentum, but not both, the individual operators can be easily evaluated using a fast Fourier transform. The split-operator method preserves the unitarity of evolutions when $D = 0$ and given a sufficient number of grid points in the spatial and momentum directions – satisfying associated Nyquist conditions – the operators can be evaluated at each timestep with essentially no spatial error.

The particular potential chosen for study was the chaotic Duffing oscillator with unit mass: $H(q, p, t) = p^2/2 + Bx^4 - Ax^2 + \Lambda x \cos(\omega t)$. The evolution was evaluated for the set of parameters $A = \Lambda = 10$, $B = 0.5$ and $\omega = 6.07$. In this parameter regime, the system is strongly chaotic, with an average Lyapunov exponent of $\bar{\lambda} = 0.57$ that is relatively uniform over the hyperbolic phase space region [41]. The size of the bounded phase space region, which is A in our calculations, is approximately 270 units of action. The hyperbolic region of the systems bounded motion is generated by the homoclinic tangle of single hyperbolic fixed point and the stable regions are relatively small. Consequently, the unstable manifold associated with this one hyperbolic point completely characterizes the chaotic region and provides an ideal test for the theory developed in this paper for bounded hyperbolic regions.

These parameters were chosen, not only because they provide appropriate testing conditions for theory, but also because their classical dynamics have been well studied in Ref. [41] and elsewhere. As a result, one can estimate the values for the order of magnitude parameters of D and t^* at which the weak version of the quantum to classical transition should occur, since the system parameters, such as $\bar{\lambda}$, are well established. In addition to the considerations due to the inequality, one also must be careful to chose a value of $\hbar$ which is not so large that the initial conditions are well outside the bounded region. Of course, choosing a value of $\hbar$ of the same order of magnitude as the bounded region or greater, would also invalidate the argument. One also does not want to choose D values which are very large compared to those at which the transition is predicted to occur, as extreme D values, while inducing quantum-classical correspondence, may wash out any interesting system dynamics.

We will principally focus on the case where $\hbar = 0.1$ for a variety of practical reasons. The value of $\hbar = 0.1$ turns out to be convenient for these purposes: the critical D value predicted is small, but not too small that it is below computational resolution, and it also allows a wide range of D values to be studied without washing out the system dynamics. This value of $\hbar$ was used in Ref. [16] which motivated much of this research, and which confirms that a weak transition will occur for this value. Still, the additional set of $\hbar$ values, $\{0.01, 0.5, 1, \sqrt{2}, 3, 5, 10, 20\}$, were studied, and all revealed similar results, though some, such as $\hbar = 0.01$ and $\hbar = 5$, had compromised dynamical ranges, while $\hbar = 10$ and 20, were too large to be of practical interest. The results presented in depth in this section for $\hbar = 0.1$ should, therefore, be thought of as emblematic of all cases studied.

The value of l_0^2 which appears in our calculation is the size of the phase space region in which our initial conditions predominantly resides. We use the same normalized initial conditions for both dual classical and quantum evolutions, as we are trying to see the degree to which the two evolutions follow each other. In the numerical simulations, the typical condition was a superposition of two Gaussians, since a classically unacceptable initial condition would better illustrate the suppression of interference effects. Other conditions were also tried and compared with analogous results.

To calculate our critical values of D and t^*, however, we used $l_0^2 = \hbar$. That is, we assume our initial condition is a minimum uncertainty wavepacket. This will give us the longest possible value of t^* necessary to terminate the development of classical structure. Making this condition larger would only make the time and effort taken to smooth over small phase space features shorter and easier. As a result our estimates represent the worst case, so that all simpler cases will be covered. For $\hbar = 0.1$, we have enough information to solve our inequalities which govern the transition. The above parameters predict that sufficient environmental coupling is present at $D \approx 0.001 - 0.01$ and that, for this value, $t^* \approx 20$.

We now set out to test whether or not this is true. We first compared the evolution at late times in order to establish whether or not a quantum-classical transition in fact occurs when we think it ought to. We started by comparing expectation values to establish the transition had occurs, but the final approval was given only after examining the distribution functions and Wigner functions

directly. Such a comparison is present in Figure 2. We compare cross sectional slices of the classical distribution function and quantum Wigner function after 149 drive periods of the Duffing oscillator. These slices are taken along the $p = 0$ line. For $D = 10^{-5}$ very little agreement occurs between the classical and quantum slices. In fact, the quantum slice still has many negative regions. By $D = 10^{-3}$, our order of magnitude estimate for when a transition should begin to occur, progress has clearly been made. The two functions are in average agreement with one another, and, though there is less agreement on the detail, there is agreement between the two on some of the larger phase space feature. By $D = 10^{-2}$, this agreement has improved. The two functions agree on most features and one can therefore say with certainty that the transition has occurred within good range of the D value predicted. This trend only improves as D continues to increase.

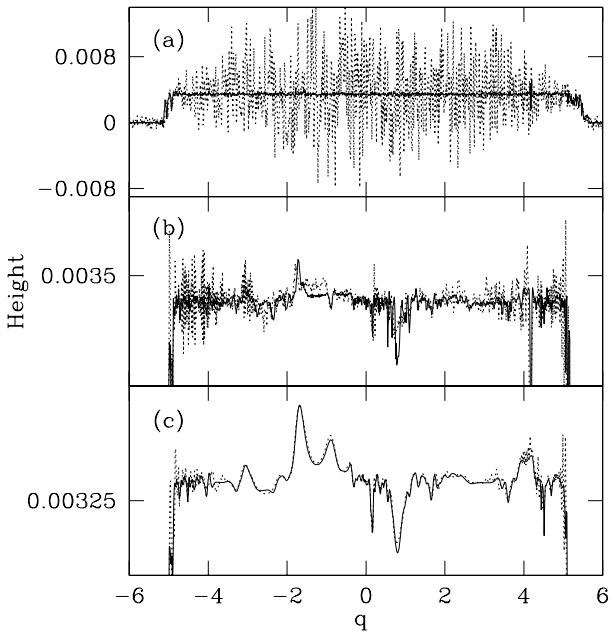

FIG. 2: Sectional cuts of Wigner functions (dashed lines) and classical distributions (solid lines) for a driven Duffing oscillator, after 149 drive periods, taken at $p = 0$ for (a) $D = 10^{-5}$; (b) $D = 10^{-3}$; (c) $D = 10^{-2}$. Parameter values are as stated in the text; the height is specified in scaled units.

Having established that the transition occured at the order of magnitude value of D predicted, we now examine if it occurs at the approximate time we expect. In Figure 3, we look at cross sectional slices taken at $t = 10$ and $t = 30$, somewhat safely on either side of the order of magnitude value of $t^* \approx 21$ we predicted. At $t = 10$, the slice in the topmost plot, the classical and quantum functions have still clearly not explored phase space sufficiently. The Wigner function, colored red, still has significant negative values and the classical distribution function has not been heavily broken up by the dynamics. By $t = 30$, shown below, the picture begins to resemble the late time plot shown in Figure 2. The negative regions have been largely eliminated and the functions are distributed throughout phase space, both settling on an average value. While there is average agreement, as in Figure 2, both disagree on the details while agreeing on some aggregate bulk features. This type of behavior continues after this time, as indicated by the previous long time slices. With reasonable allowance for error in our estimate this seems to establish that the transition has occurred close to when it is expected.

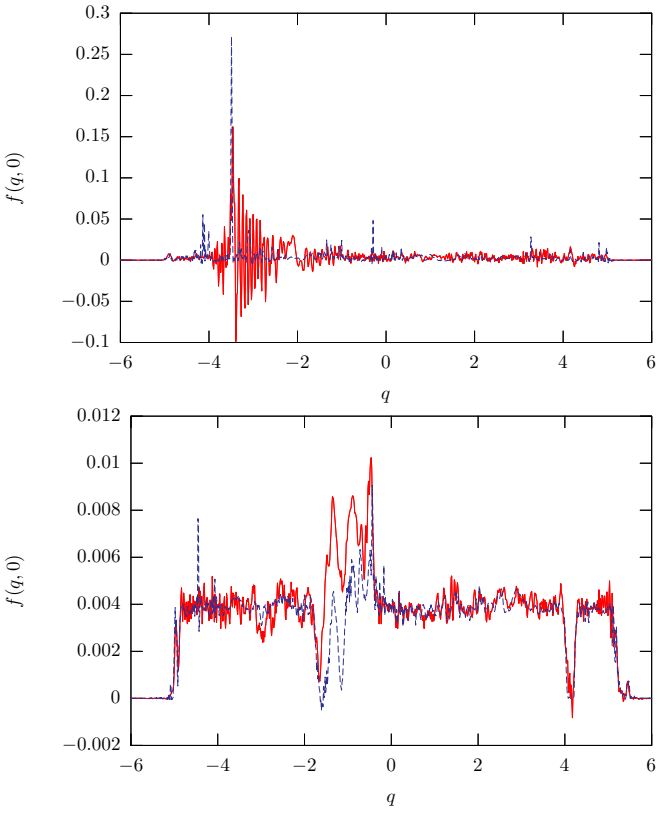

FIG. 3: Cross sectional slices of the Wigner function and classical distribution function take in phase space for $p = 0$ and $D = 10^{-3}$. The higher plot is taken at $t = 10$ and the lower plot is taken at $t = 30$. For both cases, the Wigner function slice is given in red while the classical distribution slice is blue.

To further our claim we perform a similar analysis for $D = 10^{-2}$. This is toward the end of the range of D values at which we would expect the transition to occur. Though the time at which classical structure terminates is fixed, the length at which interference is suppressed is now greater. The time at which the transition occurs here should therefore be somewhat less than the critical value explored when $D \approx 10^{-3}$. In this spirit, the topmost plot in Figure 4 looks at the case where $t = 8$ whereas the lower plot explores the $t = 20$ case. One would expect the transition to occur roughly between these two cases and in fact that is the case. As before,

the early time case shows negativity on the part of the Wigner function, but the two functions have explored phase space more fully, as expected for greater diffusion, and seem to already agree on some general features of the dynamics. The $t = 20$ case shows the strong agreement on most individual feature present in the late time case shown in Figure 2. With this in mind, along with the results of Figure 3, we can establish that the transition occurred at approximately the predicted value D and at approximately the time we predicted as well.

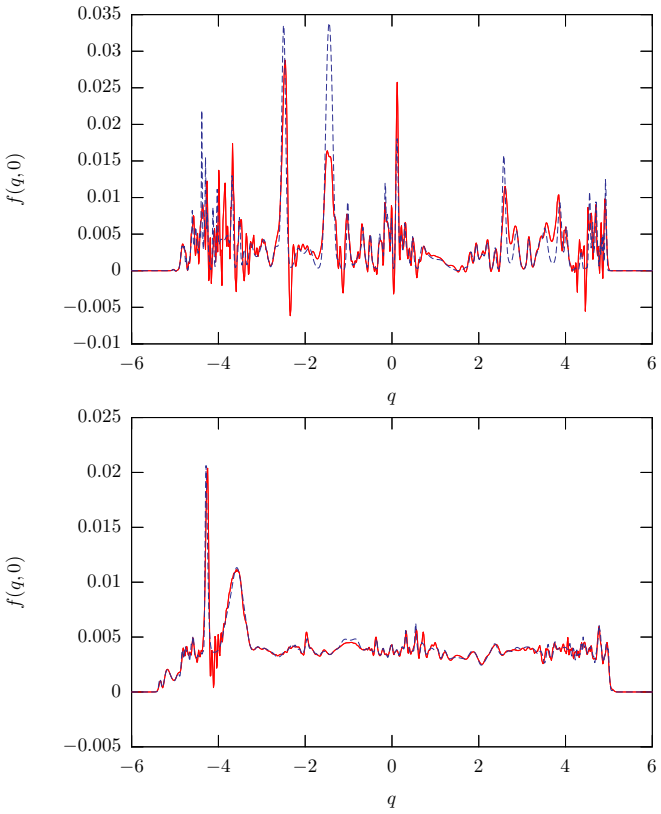

FIG. 4: Cross sectional slices of the Wigner function and classical distribution function take in phase space for $p = 0$ and $D = 10^{-2}$. The higher plot is taken at $t = 8$ and the lower plot is taken at $t = 20$. As before, the Wigner function slice is given in red while the classical distribution slice is blue.

As indicated earlier, similar results were seen at other values of $\hbar$. To sample this we show plots in Figure 5 of the $\hbar = 1$ case. The higher slice is given for $D = 0.1$ and the lower plot is given for $D = 1$. This is approximately the range at which one would expect the quantum-classical transition to occur from our criteria. Both plots are taken at $t = 20$, just after one would expect the transition to occur. In a manner similar to the previous case, and generally consistent with all cases studied, the transition begins to occur when the two functions agree on the average dynamics, while having limited agreement on the details. This is the case in the higher plot where $D = 0.1$ has a lower value, and continues to be the case at later times. In the lower plot, for the value, $D = 1$, just above the transition, there is near exact agreement, as we would expect.

These two plots also indicate some of the limitations of the approximation. Clearly, at these larger $\hbar$ values, the value of D required is also becoming larger, which will soon be inconsistent with our perturbative analytic approach. In the $D = 1$ case in Figure 5, many potentially interesting features of the dynamics are being averaged over. This is carried to an absurd extreme in Figure 6 to illustrate the point. Here we have chosen $\hbar = 20$, at which a minimum uncertainty wavepacket would begin to encroach upon the entire dynamically allowed region. The D value required is nearly 10, which is the case shown. This is a late time plot, taken at $t = 236$ and no agreement is seen. Not only is D large, but $\hbar$ is clearly so large than it has outstripped the scales which the bounded classical dynamics can explore. This reinforces that the arguments presented here only hold at reasonable physical parameter values.

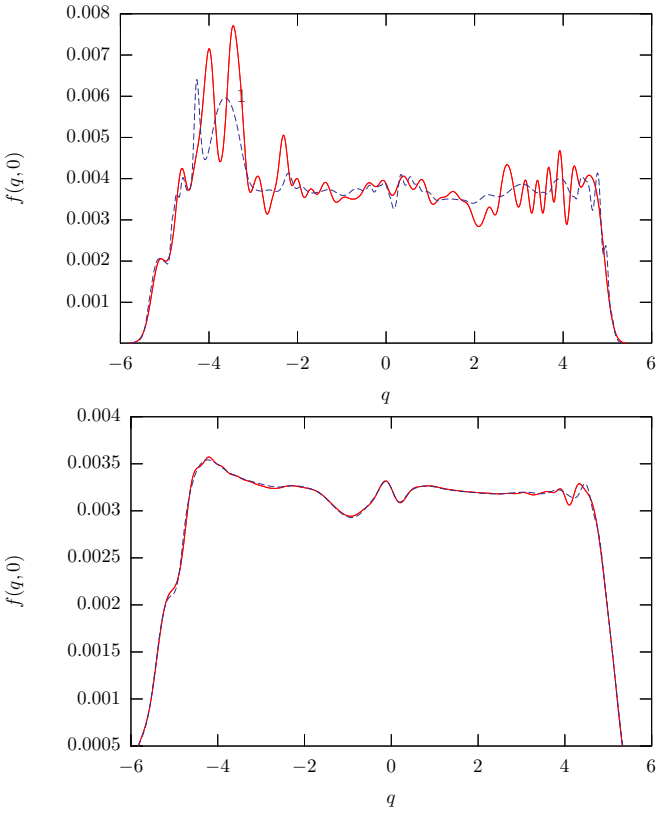

FIG. 5: Cross sectional slices of the Wigner function and classical distribution function take in phase space for $p = 0$. The higher plot is taken at $D = 0.1$ and the lower plot is taken at $D = 1$. Both are taken for at $T = 20$. Once again, the Wigner function slice is given in red while the classical distribution slice is blue.

Finally, we address one last point of the argument. It was posited that the termination of fine scale structure would lead to the presence of the early time folding associated with the foliation of the unstable manifold generated by the homoclinic point of the Duffing sys-

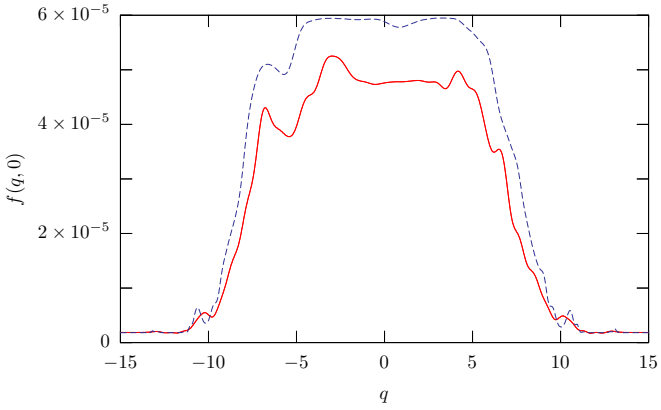

FIG. 6: A plot of the dynamics for values inconsistent with the nature of our derivation. Here $\hbar = 20$ and $D = 10$. This plot is taken at the late time of $t = 236$. As usual, quantum is red, classical blue.

tem. As evidence of this we offer in Figure 7, a full late time, high resolution phase space rendering of the Wigner function for $D = 10^{-3}$. The time is $t = 149$, well after the quantum-classical transition has occurred. Superimposed on top of it is the early time unstable manifold. Clearly, the evolution has organized along these early time features. This provides further evidence confirming our arugments for the basic mechanisms underlying the transition. The final function which both the classical distribution and Wigner function adhere to once the transition has occurred shows the suppression of the late time, fine scale features of the unstable manifold as it is supported by the large early time structures. Quantum interference, while expected, is local and is strongest near the sharp turns in the manifold where branches are most close together. This combined with the previous results in this section, allow us to conclude that the basic mechanisms posited for the quantum-classical transition are, at least approximately, correct.

The role of boundedness was important in this analysis. A bounded chaotic evolution, coupled with noise, appears to necessarily lead to the termination of fine scale structure in a chaotic evolution. In order for this analysis to be valid, the system must be bounded or, if it is unbounded, it must fold onto itself in a way which would allow a similar process to take place. The lack of such an evolution may be a reason why no such transition was found for the manifestly unbounded delta kicked rotor studied in Ref. [19].

Nevertheless, what is presented is a set of physical mechanisms which explain the source of the weak quantum-classical transition for one dimensional, bounded chaotic systems. The fact that one dimensional chaotic systems are being recovered in real world laboratory experiments, with interesting potential applications, further enhances the importance of understanding how the unconditioned environmental interactions effect a subsystem of interest. Moreover, we have used this understanding to derive order of magnitude estimates for the crossover environmental strength at which this transition occurs, as well as the time at which it occurs once this strength is met.

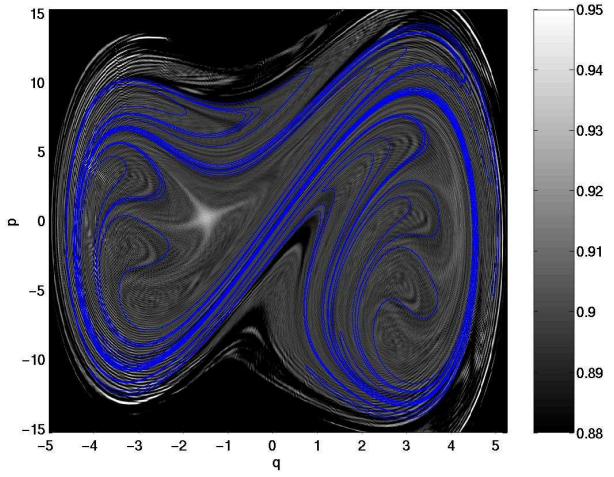

FIG. 7: Phase space rendering of the Wigner function at time $t = 149$ periods of driving. The early time part of the unstable manifold associated with the noise-free dynamics is shown in blue. The value of $D = 10^{-3}$ is not sufficient to wipe out all the quantum interference which, as expected, is most prominent near sharp turns in the manifold.

Numerical simulations were performed on the Cray T3E and IBM SP3 at NERSC, LBNL. B.D.G. and S.H. acknowledge support from the LDRD program at LANL. B.D.G. was also partially supported by the Center for Nonlinear Studies at LANL. The work of B.S. and B.D.G (partially) was supported by the National Science Foundation grant #0099431.

[1] L. Landau and E.M. Lifshitz, *Quantum Mechanics: Non-Relativistic Theory* (Pergamon Press, New York, 1965).
[2] M.V. Berry, in *Les Houches Lecture Series LIV* edited by M.-J. Giannoni, A. Voros, and J. Zinn-Justin (North-Holland, Amsterdam, 1991)
[3] A. Einstein, Verh. Dtsch. Phys. Ges. **19**, 82 (1917). M. Born, *The Mechanics of the Atom* (G. Bell, London, 1927).
[4] A.J. Dragt and S. Habib, to appear in *Proceedings of the Advanced Beam Dynamics Workshop on Quantum Aspects of Beam Physics*, (Monterey, 1998).
[5] M.V. Berry and N.L. Balazs, J. Phys. A. **12**, 625 (1979). G.P. Berman and G.M. Zaslavsky, Physica A **91**, 450 (1978). G.M. Zaslavsky. Phys. Rep. **80**, 157 (1981).

[6] S. Tomsovic and E.J. Heller, Phys. Rev. Lett. **67**, 664, (1991). Phys. Rev. E **47**, 282 (1993). arXiv:nlin.CD/0205065 (2002).

[7] J. Ford, G. Mantica, and G.H. Ristow, Physica D **50**, 493 (1991). J. Ford and G. Mantica, Am. J. Phys. **60**, 1086 (1992).

[8] D.N. Spergel, et. al, Astrophys. J. Supp. Ser. **148**, 1 (2003). Astrophys. J. Supp. Ser. **148**, 175 (2003).

[9] B.V. Chirikov, Chaos **1**, 95 (1991). S. Habib, et. al, Ann. N.Y. Acad. Sci. **1045**, 308 (2005).

[10] H.J. Carmichael, *An Open Systems Approach to Quantum Optics* (Springer, 1993); C.W. Gardiner and P. Zoller, *Quantum Noise* (Springer, 2000). M. Orszag, *Quantum Optics* (Springer, 2000).

[11] H.M. Wiseman, Ph.D. thesis, University of Queensland, 1994.

[12] S. Habib, et. al., *Proc. NATO Advanced Workshop, Nonlinear Dynamics and Fundamental Interactions*, edited by F. Khanna, (Tashkent, October 2004).

[13] C.M. Caves and G.J. Milburn. Phys. Rev. A **36**, 5543 (1987).

[14] G. Lindblad, Comm. Math. Phys. **48**, 119 (1976). V. Gorini and A. Kossakowski, J. Math. Phys. **17**, 1298 (1976).

[15] A.O. Caldeira and A.J. Leggett, Phys. Rev. E **121**, 587 (1983). A.O. Caldeira, H.A. Cerdeira, and R. Ramaswamy. Phys. Rev. A **40**, 3438 (1989).

[16] S. Habib, K. Shizume, and W.H. Zurek. Phys. Rev. Lett. **80**, 4361 (1998).

[17] T. Bhattacharya, S. Habib, and K. Jacobs, Phys. Rev. Lett. **85**, 4852 (2000).

[18] S. Habib, K. Jacobs, and K. Shizume. Phys. Rev. Lett. **96**, 010403 (2006).

[19] S. Habib, K. Jacobs, H. Mabuchi, R. Ryne, K. Shizume, and B. Sundaram, Phys. Rev. Lett. **88**, 040402 (2002).

[20] B.D. Greenbaum, S. Habib, K. Shizume, and B. Sundaram, Chaos **15**, 033302 (2005).

[21] A. R. R. Carvalho, et al., Phys. Rev. E **70**, 026211 (2004).

[22] G. Voth, G. Haller, J.P. Gollub, Phys. Rev. Lett. **88**, 254501 (2002).

[23] M.V. Berry, Phil. Trans. Royal Soc. London. A. **287**, 237 (1977).

[24] E.P. Wigner, Phys. Rev. **40**, 749 (1932).

[25] M. Hillery, R. O'Connell, M.O. Scully, and E.P. Wigner. Phys. Rep. **106**, 121 (1984). V.I. Tatarskii, 1983. Sov. Phys. Usp. **26**, 311 (1983).

[26] L. E. Ballentine, *Quantum Mechanics: A Modern Development* (World Scientific, Singapore, 1998).

[27] K. Husimi, Proc. Phys. Math. Soc. Jpn. **55**, 762 (1940).

[28] K. Takahashi and N. Sait, Phys. Rev. Lett. **55**, 645 (1985). D. Lalovič, D. M. Davidović, and N. Bijedić, Phys. Rev. A **46**, 1206 (1992).

[29] W.H. Zurek and J.P. Paz. Phys. Rev. Lett. **72**, 2508 (1994). Physica D, **83**, 300 (1995).

[30] R.L. Hudson, Rep. Math. Phys. **6**, 249 (1974).

[31] E.J. Heller, J. Chem. Phys. **67**, 3339 (1977).

[32] For example, L.I. Schiff, *Quantum Mechanics* (McGraw-Hill, New York, 1968), 3rd ed. B.H. Brandsen and C.J. Joachain, *Introduction To Quantum Mechanics* (Prentic Hall, New York, 2000).

[33] V.P. Maslov and M.V. Fedoriuk, *Semi-Classical Approximation in Quantum Mechanics* (Dordrecht, Holland, 1981).

[34] C. Bender and S. Orszag, *Advanced Mathematical Methods for Scientists and Engineers* (Mc-Graw Hill, New York, 1978).

[35] G. Chester, B. Friedman, and F. Ursell, Proc. Camb. Phil. Soc. **53**: 599 (1957).

[36] C.W. Gardiner, *Handbook of Stochastic Methods* (Springer-Verlag, Berlin, 1997).

[37] N.G. Van Kampen, *Stochastic Processes in Physics and Chemistry* (Elsevier North Holland, New York, 1983).

[38] W. Liu and G. Haller, Physica D. **188**: 1 (2004).

[39] A.R. Kolovsky, Phys. Rev. Lett. **76**: 340 (1996).

[40] M.D. Feit, J.A. Fleck, Jr., and A. Steiger, J. Comp. Phys. **47**, 412 (1982).

[41] W.A. Lin and L.E. Ballentine, Phys. Rev. Lett. **65**, 2927 (1990).